

Phonon spectrum of a model of electronically excited silicon

Rana Biswas and Vinay Ambegaokar

Laboratory of Atomic and Solid State Physics, Cornell University, Ithaca, New York 14853

(Received 2 March 1982)

With a view to clarifying the process proposed in the plasma-annealing hypothesis for laser-induced recrystallization, we have performed a simple calculation of phonon frequencies in electronically excited silicon. We make assumptions most favorable to the plasma-annealing hypothesis, i.e., we assume that the laser energy remains in the electronic system. We use a one-parameter interpolation of the electronic dielectric constant between the bond charge and the free-electron models in a computation of the phonon spectrum. The calculation yields a softening of the [111] *zone-boundary* transverse-acoustic phonons. Typically, such a softening would be thought to lead to a structural phase transition. The excited electron densities needed for this softening are in the range $(6-10) \times 10^{21} \text{ cm}^{-3}$ which seems unreasonably large to us. Thus, on two counts, we have grounds for rejecting the plasma-annealing hypothesis.

I. INTRODUCTION

In this paper we calculate the phonon spectrum of silicon containing a high density of excited electron-hole pairs. Our purpose is to clarify the process proposed in the plasma-annealing hypothesis for laser-induced recrystallization in semiconductors.

Laser annealing is an established technique for obtaining high-quality crystalline and defect-free material from radiation-damaged silicon samples.¹ Laser beams with typical pulse lengths of 10–20 ns and energy densities $1-2 \text{ J cm}^{-2}$ are used in this process.²⁻⁶ The majority of pulsed laser experiments provide evidence for a thermal melting process in the semiconductor followed by recrystallization into a relatively defect-free structure.³⁻⁷

The plasma-annealing hypothesis has been proposed as an alternate explanation of these phenomena.⁸ In this hypothesis, the laser pulse creates a dense ($> 10^{21} \text{ cm}^{-3}$) electron-hole plasma, and it is proposed that the bulk of the excitation energy remains in the electron system during the annealing process.⁸⁻¹⁰ Under these conditions of high electronic excitation it is proposed that the crystal loses its resistance to shear because the transverse acoustic (TA) phonon modes become unstable.⁸ The material then enters a "cold fluid" phase where the ions are soft against shear and defects can easily diffuse away. Comparatively little basic work has been done to elucidate the mechanism of the proposed plasma-annealing process.

Some motivation for the plasma-annealing model

stems from an earlier calculation by Martin of phonon frequencies in silicon.¹¹ There the electrons were first described by a free-electron gas (with free-electron screening) only to obtain unstable TA phonon modes. Then the effects of the covalent binding were included, through bond charges, to obtain stable phonon modes in reasonable agreement with experiment.

We calculate the phonon spectrum of electronically excited silicon within a simple model. We assume that the excited electron-hole plasma retains the major portion of the excitation energy, with negligible energy transfer to the lattice. This assumption permits a simple calculation of phonon dispersion curves. More sophisticated models would contain many additional parameters. More importantly, we note that the above assumption is the *most favorable* for the plasma-annealing hypothesis. If the predictions of the plasma-annealing hypothesis are untenable in these circumstances, they should be untenable in any physical situation.

Within this framework, the adiabatic approximation still holds, allowing a description of the electronic response by a static dielectric function. In our model the electronic dielectric function is a one-parameter interpolation between the bond-charge and the free-electron models.

The results of our calculation show that up to an excited electronic density of 10^{21} cm^{-3} there is essentially no change in the phonon spectrum. Beyond 10^{21} cm^{-3} the TA phonon modes change dramatically, with the zone-boundary TA phonons

going soft. It is the zone-boundary TA phonon in the [111] direction which becomes unstable first, i.e., its frequency becomes imaginary, the transition occurring at the large density of $N_e \simeq 9 \times 10^{21} \text{ cm}^{-3}$.

The proponents of the plasma-annealing theory imply that the entire TA mode becomes unstable,¹² leading to a fluidlike phase. In this hypothesis, the sound velocities (or the slopes of the phonon curves at $q \rightarrow 0$) would decrease to zero at the transition. This does not happen in our calculations. In short, even when we accept the notion that the electronic system retains the excitation energy during much of the annealing process—a notion that is hard to justify—we do not obtain the postulated fluid phase.

This paper is organized into five sections. The following section discusses the main features of our model. First the relevant time scales in the problem are discussed and then the electronic dielectric function of the excited semiconductor is constructed. Section III deals with the dynamical matrix calculations within the framework of the bond-charge model. Section IV presents the results of our calculation of the phonon spectrum. Section V contains concluding remarks, including comments about the relevance of the calculation to structural transitions in other diamond-structure crystals.

II. THE MODEL

A. Microscopic time scales

In our calculation of the lattice dynamics of electronically excited silicon we will implicitly assume the validity of the inequalities

$$\omega_{\text{pl}} > \omega_{\text{ph}} > \frac{1}{\tau_{e\text{-ph}}}, \frac{1}{\tau_{\text{diff}}}. \quad (1)$$

Here ω_{pl} is the plasma frequency of the electronic system, typically 10^{15} s^{-1} ; ω_{ph} is a typical phonon frequency ($\sim 10^{12} - 10^{13} \text{ s}^{-1}$); $\tau_{e\text{-ph}}$ is the electron-phonon relaxation time (quoted to be in the range $10^{-10} - 10^{-12} \text{ s}$ (Refs. 13–15)); and τ_{diff} is approximately the time for a carrier to diffuse one absorption depth. The inequality $\omega_{\text{ph}} > 1/\tau_{e\text{-ph}}, 1/\tau_{\text{diff}}$ implies that any typical electronic state remains coherent and is not scattered in a few time periods of the lattice vibration.

We emphasize that it is difficult to justify these inequalities under highly excited conditions. As already mentioned, we are suspending judgment on this question in order to give the plasma-annealing hypothesis its best chance. Assuming the inequali-

ties permits us to treat the electrons as following the ionic motion adiabatically. The response of the electron system is then described by the *static* dielectric functions $\epsilon(q, \omega=0)$ and $\epsilon(q+G, q+G', \omega=0)$.

Under the stated assumptions, the carrier temperatures become comparable with the band-gap energy, i.e., $k_B T_e \simeq E_g$. Then the Auger and the inverse Auger processes have equal probabilities, with detailed balance maintained between them. The Auger process, and the electron-electron interaction⁹ in general, are then thermalization processes for the *e-h* plasma, redistributing energy within the electronic system.

Other authors, in particular Combescot,¹⁶ have considered the opposite point of view where the electron-phonon interaction is strong enough to maintain thermal equilibrium between the electrons and the lattice. Then the Auger process is the dominant mode for recombination of the carriers and it limits the total excited electronic density possible in the semiconductor.¹⁶

The electron-phonon relaxation time $\tau_{e\text{-ph}}$ has been stated to be $\sim 10^{-10} - 10^{-12} \text{ s}$, being uncertain to an order of magnitude because of the inaccurately known electron-phonon coupling strength. Yoffa¹⁷ has examined the effect of high excitations on this time $\tau_{e\text{-ph}}$. She finds that up to $10^{20} - 10^{21} \text{ cm}^{-3}$ there is no appreciable decrease in the phonon emission rate, though screening effects do decrease this rate at higher densities.

Carrier diffusion reduces the density of excited electrons. Times of $\tau_{\text{diff}} \approx 100 \text{ ps} = 10^{-10} \text{ s}$ have been estimated¹³ for a carrier to diffuse over one absorption depth ($\sim 1 \mu\text{m}$).

B. The dielectric function

Much of the following procedure, especially the phonon spectrum calculations of Sec. III, closely follows the analysis of Martin.¹¹

To describe the response of the electronic system we note that the dielectric function in a semiconductor is a tensor $\epsilon(q+G, q+G')$.^{18,19} The off-diagonal components of the dielectric function are essential for charge neutrality in the semiconductor. The diagonal dielectric constant remains finite in the long-wavelength limit $\epsilon(q) = \epsilon(q, q) \rightarrow \epsilon_0$, indicating that the ionic charge is incompletely screened. The remaining charge may be associated with the covalent bonds in the semiconductor.^{18–20}

In a first attempt to compute phonon dispersion relations in silicon, Martin, in applying the well-

known formalism of phonons in metals, treated the electrons as a free-electron gas, described through a metallic dielectric function: $\epsilon(q) \underset{q \rightarrow 0}{\sim} 1 + k_s^2/q^2$.

This produced unstable transverse-acoustic (TA) phonon modes with all the TA frequencies imaginary.¹¹ Then the effects of the off-diagonal charge screening were approximated by the bond-charge model. This model introduces static bond charges, lying midway between the ions. These charges are localized point charges which are always constrained to lie midway between the ions, even when the ions are displaced. Along with a semiconductorlike dielectric function, the bond-charge model produced stable phonon modes, in

$$\epsilon(q) = 1 + \frac{4\pi e^2}{q^2} \sum_k \sum_G \frac{f^0(k) - f^0(k+q+G)}{E(k+q+G) - E(k)} |\langle k | e^{i\vec{q} \cdot \vec{r}} | k+q+G \rangle|^2 \quad (2)$$

in the extended zone scheme of the semiconductor, $f_0(k)$ being the distribution function of the Bloch state $|k\rangle$ of energy $E(k)$.

For the ground state $T=0$ semiconductor (filled valence band), the dielectric constant in the long-wavelength limit has been estimated using (2) and a two-band model of a semiconductor to be^{21,22}

$$\epsilon_g(q) \underset{q \rightarrow 0}{\simeq} 1 + \frac{4\pi N_0 e^2 \hbar^2}{m (E_{\text{gap}})^2} = 1 + \left(\frac{\hbar \omega_{pl}}{E_{\text{gap}}} \right)^2. \quad (3)$$

N_0 is the total electronic density and E_{gap} a parameter approximating the average difference between states in the two bands lying vertically above each other.

For Si, the parameter we use are $N_0 = 2.00 \times 10^{23} \text{ cm}^{-3}$, $E_{\text{gap}} \simeq 5.01 \text{ eV}$, which yield the experimental value of $\epsilon_0 \simeq 12.0$.

We have constructed a dielectric function that describes the semiconductor Si with N_e e - h pairs excited in it. In the long-wavelength limit, we generalize (3):

$$\epsilon(q) \underset{q \rightarrow 0}{\simeq} 1 + \frac{k_s^2}{q^2} + \frac{4\pi(N_0 - N_e)e^2 \hbar^2}{m (E_{\text{gap}})^2}, \quad (4)$$

where k_s is a screening length, discussed later in this section. We have an approximate analysis to support Eq. (4). However, for the purposes of the following calculation it suffices to note that this form is a one-parameter linear interpolation of the long-wavelength dielectric function between the bond-charge model and the free-electron limit. For the ground-state semiconductor, $N_e = 0$, $k_s = 0$, $\epsilon(q)$ reduces as it should to ϵ_0 , while for the highly excited case ($N_e \approx N_0$), $\epsilon(q)$ approaches the free-

reasonable agreement with experiment.

We are modifying Martin's calculations in this paper, and interpolating between the two-limits—the bond-charge model which describes the ground-state semiconductor and the free-electron model which describes the state with all the electrons excited. In particular, we investigate the way in which a stable TA phonon mode is destabilized by excited carriers, and is transformed into the unstable mode of the free-electron limit.

The diagonal part of the dielectric function $\epsilon(q)$ is expressed within the random-phase approximation (RPA) as

electron limit,

$$\epsilon(q) \approx 1 + \frac{k_s^2}{q^2}.$$

Physically one might expect a linear interpolation between the two limits rather than a more complicated functional form since whatever charge N_e is excited out of the bands is distributed uniformly as a free-electron gas of the same density N_e , maintaining charge conservation. Further, sum rules restrict the interband dielectric constant to be proportional to the number of filled valence-band states [which is $(N_0 - N_e)$ here].

We extend the dielectric function in (4) to finite wave vector q as follows. First we note that the third term in (4), $4\pi(N_0 - N_e)e^2 \hbar^2 / m (E_{\text{gap}})^2$, arises from the virtual interband transitions of the general expression (2). The analogous term in the ground-state semiconductor, $4\pi N_0 e^2 \hbar^2 / m (E_{\text{gap}})^2$, also arises from these same virtual transitions from the valence to the conduction band. For finite wave vectors these two interband terms should have the same q dependence. In particular, we make use of the known dielectric function $\epsilon_g(q)$ (Refs. 11 and 23) for the ground-state semiconductor and scale the magnitude of $[\epsilon_g(q) - 1]$ with the factor $(N_0 - N_e)/N_0$ to obtain the interband form when $N_e \neq 0$.

The k_s^2/q^2 form of the screening of the e - h plasma is retained at finite q . This procedure provides the dielectric function:

$$\epsilon(q) \simeq 1 + \frac{k_s^2}{q^2} + [\epsilon_g(q) - 1] \left[\frac{N_0 - N_e}{N_0} \right]. \quad (5)$$

As expected, $\epsilon(q) \rightarrow 1$ at large q . We have also tried slightly different functional forms for $\epsilon_g(q)$ and found that the phonon frequencies are not sensitive to these changes.

To complete the specification of the dielectric constant (5) we must express k_s in terms of N_e . One way of doing this, which is in the spirit of our basic assumption of electron thermalization, is to characterize the plasma by a temperature T_e . We can then relate the temperature T_e to the density N_e of excited electrons through the equation

$$N_e = \int_0^\infty \frac{g_0(E)dE}{1 + \exp[(E - \mu)/k_B T_e]} \quad (6)$$

Defining the Fermi integral

$$F_{1/2}(\alpha) = \int_0^\infty \frac{x^{1/2} dx}{e^{(x-\alpha)} + 1} \quad (7)$$

and

$$n_0^e(T_e) = \frac{1}{4} \left[\frac{2m_e^* k_B T_e}{\pi \hbar^2} \right]^{3/2} \quad (8)$$

we obtain (noting that there are six equivalent conduction-band minima in Si)

$$N_e(T_e) = \frac{2}{\pi^{1/2}} n_0^e(T_e) 6F_{1/2}(\alpha) \quad (9)$$

with

$$\alpha = \frac{\mu - E_c}{k_B T_e} \quad \text{and} \quad \beta = \frac{E_V - \mu}{k_B T_e}.$$

We equate the number of holes to that of electrons

($N_e = N_h$) to obtain

$$6 \left[\frac{m_e^*}{m_h^*} \right]^{3/2} F_{1/2}(\alpha) = F_{1/2}(\beta) \quad (10)$$

with

$$\alpha + \beta = \frac{-E_g}{k_B T_e}. \quad (11)$$

E_g is the energy gap which we assume does not vary much with N_e or T_e . This is justified since at high temperatures T_e , $k_B T_e \geq E_g$, and the above equations are then not so sensitive to E_g .⁹

Solving the two coupled equations (10) and (11) we obtain the chemical potential μ and the density N_e as a function of T_e which is plotted in Fig. (1). This is the same curve as was obtained by Yoffa.⁹

Further we plot $k_B T_F$, the Fermi energy of the e - h plasma treating it as a free Fermi gas, against $k_B T_e$ in Fig. (2). The graph shows that $T_e > T_F$ for all ranges of N_e , so that the dense e - h plasma can be treated as a classical gas obeying a Boltzmann distribution of temperature T_e .

The screening in the dielectric function $\epsilon(q)$ can then be described by the Debye Huckel formula

$$k_s^2 = \frac{4\pi(2N_e)e^2}{k_B T_e}, \quad (12)$$

the screening of a hot classical gas of temperature T_e .

The dielectric constant (5), with k_s determined by Eq. (12), has been used to obtain the results presented in Sec. IV. It may be worth mentioning

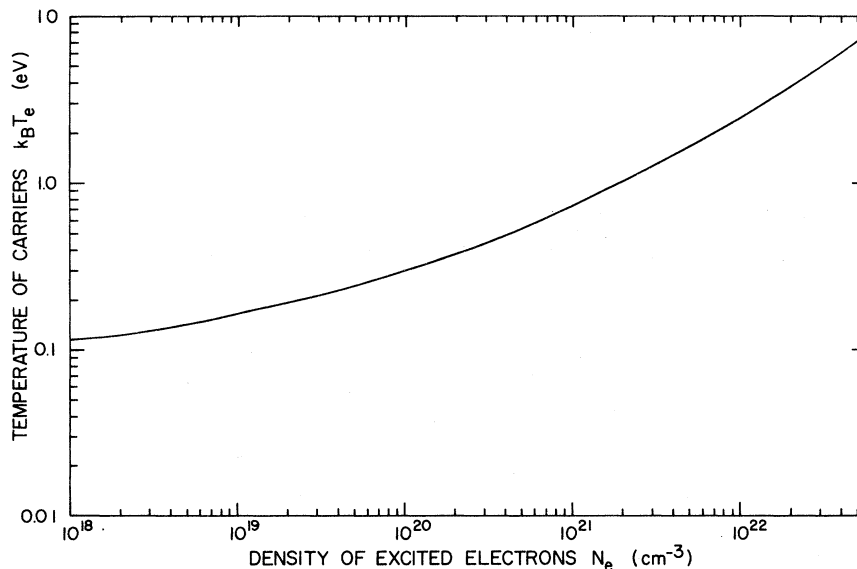


FIG. 1. Temperature of the excited carriers $k_B T_e$ as a function of the excited electron density N_e .

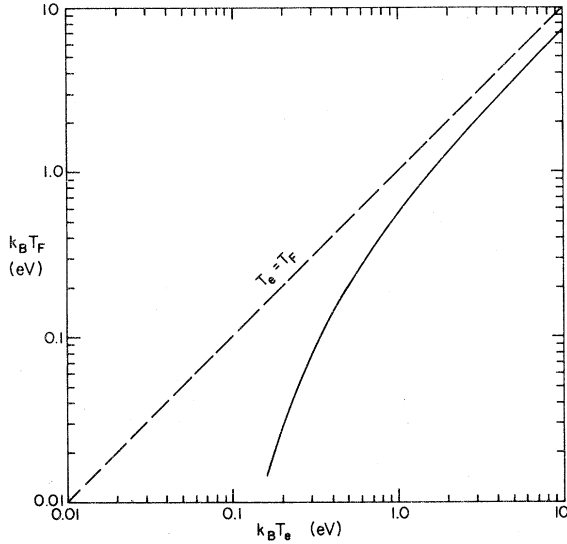


FIG. 2. Fermi energy of the excited e - h plasma $k_B T_F$ (treated as a free Fermi gas) as a function of the carrier temperature $k_B T_e$.

that the calculated phonon curves do not depend crucially on the assumption of a hot classical plasma as in (12). Qualitatively similar results are obtained on the assumption that the screening is due to degenerate electron and hole plasmas.

$${}^{(1)}C_{ss'}^{\alpha\beta}(q; N_e) = \frac{\Omega}{4\pi e^2} \sum_{\mathbf{G}} (q + \mathbf{G})_{\alpha} (q + \mathbf{G})_{\beta} |q + \mathbf{G}|^2 |v(q + \mathbf{G})|^2 \left[\frac{1}{\epsilon(q + \mathbf{G})} - 1 \right] e^{i\vec{G} \cdot (\vec{R}_s - \vec{R}_{s'})} + \frac{4\pi e^2}{\Omega} Z^2 G_{\alpha\beta}(q, R_s - R_{s'}) \quad (15)$$

with

$$\epsilon(q + \mathbf{G}) = 1 + \frac{k_s^2}{|q + \mathbf{G}|^2} + [\epsilon_g(q) - 1] \left[\frac{N_0 - N_e}{N_0} \right], \quad (16)$$

$$G_{\alpha\beta}(q, R_s - R_{s'}) = - \sum_l' f_{\alpha\beta}(R_s - R_l - R_{s'}) \exp[-i\vec{q} \cdot (\vec{R}_s - \vec{R}_{s'} - \vec{R}_l)], \quad (17)$$

and

$$f_{\alpha\beta}(r) = \frac{\partial^2}{\partial r^{\alpha} \partial r^{\beta}} \left[\frac{1}{|r|} \right]. \quad (18)$$

Here $f_{\alpha\beta}(r)$ describes the Coulomb interaction; (l, s) denotes the s th basis atom in the l th unit cell and Ω is the volume of the primitive cell. Further, $R_s' = \frac{1}{4}a(1, 1, 1)$, where $a = 5.43 \text{ \AA}$.

$G_{\alpha\beta}(q, R_s - R_{s'})$ is evaluated by the Ewald transformation.

The contribution that the off-diagonal elements $\epsilon^{-1}(q + \mathbf{G}, q + \mathbf{G}')$ make to the dynamical matrix

III. PHONON FREQUENCIES

The phonon dispersion relations in our model are obtained by diagonalizing a 6×6 dynamical matrix $D(q)$ in different directions in the first Brillouin zone to obtain the frequencies $\omega_s^{\alpha}(q)$. Translational invariance implies that^{11,24}

$$D_{ss'}^{\alpha\beta}(q) = \frac{1}{(M_s M_{s'})^{1/2}} \left[C_{ss'}^{\alpha\beta}(q) - \delta_{ss'} \sum_{s''} C_{ss''}^{\alpha\beta}(0) \right], \quad (13)$$

$$D_{ss'}^{\alpha\beta}(q) e_s^{\beta}(q) = \omega_s^{\alpha 2}(q) e_s^{\alpha}(q). \quad (14)$$

Here $\alpha, \beta (= 1, 2, 3)$ are the Cartesian components $s, s' (= 1, 2)$ the labels for the basis atoms, and M is the mass of the Si ion.

We calculate the dynamical matrix by generalizing Martin's analysis¹¹ to include the screening effect discussed in the last section. The first contribution to the matrix $C_{ss'}^{\alpha\beta}(q)$ is analogous to that in a metal. It contains the electronic contribution to the dynamical matrix where the electron-ion interaction is described through an ion-core potential $v(q)$, and screened by the dielectric function $\epsilon(q)$ from (5). The ion-core potential is the same as used by Martin.¹¹ Also, the "Madelung" energy of the bare ions ($Z=4$) is added to the electronic contribution. So ${}^{(1)}C_{ss'}^{\alpha\beta}(q; N_e)$ is

are approximated within the *bond-charge model*, by the Coulomb interactions between bond charges and ions.

In the ground state since Z/ϵ_0 of the electronic charge is not used in linear screening, charge conservation provides the magnitude of the bond charge Z_b . Counting the total electronic charge per atom,

$$(Z - Z/\epsilon_0) + 2Z_b = Z, \quad (19)$$

$$Z_b = \frac{Z}{2\epsilon_0} = \frac{1}{6}. \quad (20)$$

The interaction between the static charges is pure Coulombic [$u(r) \propto 1/r$].

Exciting a density N_e of electrons depletes the magnitude of the bond charge. We rewrite the dielectric function (4) as

$$\begin{aligned} \epsilon(q) &\simeq_{q \rightarrow 0} 1 + \frac{k_s^2}{q^2} + \frac{4\pi(N_0 - N_e)e^2\hbar^2}{m(E_{\text{gap}})^2} \\ &= \epsilon'_0 + \frac{k_s^2}{q^2}. \end{aligned} \quad (21)$$

ϵ'_0 describes the semiconductorlike dielectric constant which linearly screens the ions. Once again

using charge conservation, and counting the electronic charge per atom,

$$(Z - Z/\epsilon'_0) + \frac{N_e}{N_A} + 2Z'_b = Z, \quad (22)$$

$$Z'_b = \frac{Z}{2\epsilon'_0} - \frac{N_e}{2N_A}. \quad (23)$$

Here Z'_b is the new bond charge and N_A is the atomic density of Si ($=N_0/4$).

The contribution of the bond charges to the dynamical matrix ${}^{(2)}C_{ss}^{\alpha\beta}(q; N_e)$ is then

$$\begin{aligned} {}^{(2)}C_{ss}^{\alpha\beta}(q; N_e) &= -e^2 \sum_{i,j=1}^5 (WZ)_{ij} [\exp\{i\vec{q} \cdot [\vec{R}_i(s) - \vec{R}_j(s')]\} G'_{\alpha\beta}(q, R_s + R_i(s) - R_{s'} - R_j(s')) \\ &\quad - (1 - \delta_{ss'})(1 - \delta_{i,5}) e^{2i\vec{q} \cdot \vec{R}_i(s)} G'_{\alpha\beta}(0, R_i(s) - R_j(s))], \end{aligned} \quad (24)$$

where $i = j = 5$ is excluded and where

$$\begin{aligned} W_i &= \frac{1}{2}, \quad Z_i = \epsilon'_0 Z'_b \quad (i \leq 4) \\ W_i &= 1, \quad Z_i = 4 \quad (i = 5). \end{aligned} \quad (25)$$

$R_i(s)$ are the bond-charge positions about ion s for $i \leq 4$ and $R_5(s) = 0$. $R_i(s)$ are

$$\begin{aligned} R_1(1) &= -R_1(2) = \frac{1}{8}a(1, 1, 1), \\ R_2(1) &= -R_2(2) = \frac{1}{8}a(1, -1, -1), \\ R_3(1) &= -R_3(2) = \frac{1}{8}a(-1, 1, -1), \\ R_4(1) &= -R_4(2) = \frac{1}{8}a(-1, -1, 1). \end{aligned} \quad (26)$$

$G'_{\alpha\beta}$ in (24) is defined through

$$G'_{\alpha\beta}(q, r) = \sum_I f'_{\alpha\beta}(r - R_I) e^{-i\vec{q} \cdot (\vec{r} - \vec{R}_I)}. \quad (27)$$

Here the density N_e of excited electrons provides a screening medium of wave vector k_s . $f'_{\alpha\beta}$ is the screened Coulomb interaction,

$$f'_{\alpha\beta}(r) = \frac{1}{\epsilon'_0} \frac{1}{r} e^{-k'_s r}, \quad (28)$$

$$k'_s = \frac{k_s}{\sqrt{\epsilon'_0}}. \quad (29)$$

$G'_{\alpha\beta}$ was also calculated with an Ewald sum for the screened Coulomb interaction. Finally,

$$C_{ss}^{\alpha\beta}(q; N_e) = {}^{(1)}C_{ss}^{\alpha\beta}(q; N_e) + {}^{(2)}C_{ss}^{\alpha\beta}(q; N_e) \quad (30)$$

The $q = 0$ part of the dynamical matrix is well

behaved as is evident from the above formalism, ensuring the charge neutrality of the system.

The dynamical matrix $D_{ss}^{\alpha\beta}(q; N_e)$ was constructed and then diagonalized to find the dispersion curves at different excited densities N_e .

More sophisticated schemes to calculate phonons in semiconductors are available.^{25,26} However we choose the present scheme because it allows an intuitively appealing way of adding excited carriers, which the more elaborate bond-charge models²⁶ do not.

IV. RESULTS

The phonon dispersion relations were calculated along the [100], [110], and [111] symmetry directions, for a range of excited electronic densities, as plotted in Fig. (3). The results are summarized by the following points.

(1) For the ground-state semiconductor, i.e., $N_e = 0$, our calculations agree with the earlier results of the bond-charge model for Si.¹¹ The flat TA modes are a characteristic feature of group-IV semiconductors [See note added in proof.]

(2) Increasing N_e up to 10^{21} cm^{-3} resulted in negligible changes in the phonon frequencies. At 10^{21} cm^{-3} the TA mode was slightly raised due to the change in $\epsilon(q)$ affecting the electronic contribution in (25).

(3) Raising N_e beyond 10^{21} cm^{-3} produced dramatic effects in the TA modes. The zone-boundary TA frequencies decreased rapidly with

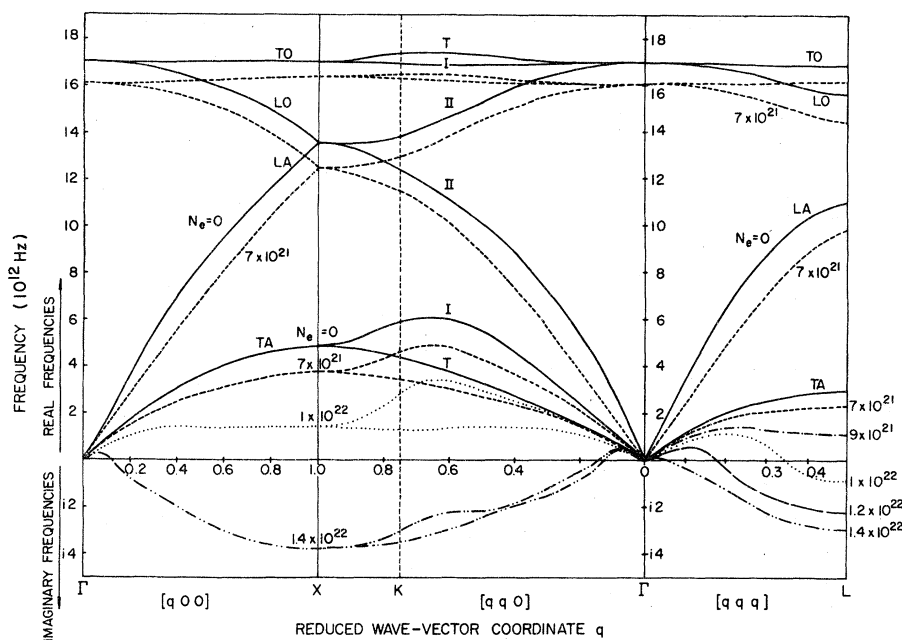


FIG. 3. Phonon spectrum at different excited electronic densities N_e . The solid curves are for the unexcited system and the dashed curves for the different excited densities indicated. The longitudinal and the optic modes for 1×10^{22} are very similar to those at 7×10^{21} and have been omitted.

increasing N_e , although the long-wavelength phonon frequencies were not altered much. It is the zone-boundary phonon at the [111] zone boundary $[\omega_{TA}(L)]$ which first becomes unstable. A graph

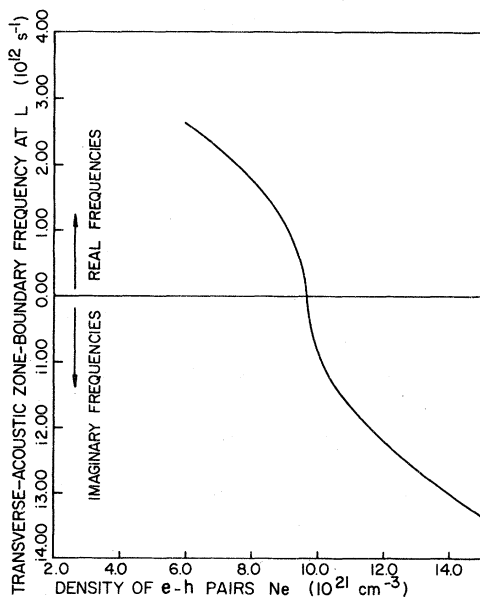


FIG. 4. Zone-boundary TA phonon frequency at L as a function of the excited electronic density, showing the zone-boundary mode softening. The frequency goes to zero at $N_e \sim 9 \times 10^{21} \text{ cm}^{-3}$ and becomes imaginary beyond this density.

of $\omega_{TA}(L)$ vs N_e , Fig. (4), shows that the transition is a very sharp one, the instability occurring at a density $N_e^{\text{crit}} \sim 9 \times 10^{21} \text{ cm}^{-3}$ which corresponds to $\sim 4.5\%$ of the total electronic charge. Most importantly, we note that at the transition point, only *one* phonon mode, the [111] TA mode at L , is unstable, while all other phonon modes are stable.

(4) Beyond the critical density N_e^{crit} , the calculation has no obvious meaning but we did check that we obtained agreement with Martin's free-electron limit. For N_e greater than N_e^{crit} a larger portion of the TA mode, from the zone-boundary inwards, is unstable, until the entire TA mode destabilizes in the $N_e \simeq N_0$ free-electron limit.

(5) Examining the different contributions to the dynamical matrix, we find that the rapid decrease in the zone-boundary frequencies above $N_e \sim 10^{21} \text{ cm}^{-3}$ is due to the depletion of the bond-charge magnitude Z_b , which occurs significantly only when N_e is some macroscopic fraction of N_0 , the total electronic density. This happens roughly when N_e exceeds 10^{21} cm^{-3} . According to Eq. (26) which expresses the functional dependence of Z_b on N_e , the bond-charge magnitude Z_b vanishes for $N_e \geq 1.8 \times 10^{22} \text{ cm}^{-3}$. However the instability occurs well before we reach this point.

(6) With increasing N_e , the optic modes become more free-electron-like with $\omega_{TO}(q)$ increasing, as q increases from the zone center towards the zone

boundary.

(7) Calculations were performed with different choices for the ion-core potential $v(q)$ and the dielectric function $\epsilon_g(q)$. It was found that the relevant physical features of the phonon spectrum and the TA mode softening remain the same, though the actual numerical value of N_e^{crit} changes with different $v(q)$ or different $\epsilon_g(q)$. From these calculations a reasonable value of N_e^{crit} could lie in the range $(6-10) \times 10^{21} \text{ cm}^{-3}$. For definiteness we show the results of a particular set of calculations in Fig. (3) which produced $N_e^{\text{crit}} \simeq 9 \times 10^{21} \text{ cm}^{-3}$.

V. CONCLUDING REMARKS

We undertook this calculation because we were intrigued by the plasma-annealing hypothesis of a nonequilibrium solid in which the lattice loses shear resistance because of electronic excitation. Our calculations do not support this idea, giving a zone-boundary mode softening instead. This mode-softening effect might, if at all, occur in highly transient situations or on very short time scales ($\simeq 1$ ps), where the nonequilibrium conditions of our model could be realized. We doubt very much that this effect occurs in photoexcited silicon with the usual annealing pulses.

Our calculation has the merit of being complete and well defined. The key ingredients for the transverse-acoustic mode softening are the weakening of bond charges and a corresponding metallic screening. The assumptions of small electron-phonon scattering and electron thermalization are a way of achieving these ingredients.

It is tempting to speculate that our calculation contains some of the physics of the well-known temperature-induced transition in tin—from the α (i.e., diamond structure) form to the β -tetragonal metallic phase at 13° C . A superposition of [111] shears has been identified as the displacement needed for this structural change.²⁷ Since α -tin is a semimetal with a zero direct band gap, electronic

excitations are energetically inexpensive. The process we have calculated can, however, only be part of the explanation of this transition because (i) the transition is first order with a 21% increase in density in the β phase, and (ii) though the shear modes of α -tin are already quite soft, further mode softening near the transition has not been reported. It is possible that our process signals a second-order transition which is overtaken by a first-order one, in which case the mode softening should be evident in superheated α -tin. We intend to study further both this transition and other structural “metallization” transitions in diamond-structure crystals.^{28,29}

Note added in proof. Small differences between our $N_e = 0$ curves and the modes calculated by Martin in Ref. 11 are due to slightly different inputs. The results shown in our Fig. 3 above do not include an “exchange correction” to the dielectric function, with the consequence that our TA modes are somewhat softer than Martin’s. Since the two calculations bracket the experimental [111] zone-boundary TA frequency, the refinement has no obvious advantages for our purposes. However, in recent calculations, we have closely matched Martin’s results for the unexcited system. On excitation, the characteristic mode softening described above again results, with N_e^{crit} being somewhat higher, presumably because one starts with stiffer modes.

ACKNOWLEDGMENTS

We thank R. M. Martin for helpful suggestions and for providing us with tabulated values of the dielectric function and the ion-core potential. Useful discussions with G. Barsch, A. Carlsson, M. E. Fisher, R. Pandit, J. A. VanVechten, J. W. Wilkins, and E. J. Yoffa are gratefully acknowledged. We were supported in part by the National Science Foundation under Grant No. DMR-80-20429.

¹*Laser and Electron Beam Processing of Materials*, edited by C. W. White and P. S. Peercy (Academic, New York, 1980).

²I. B. Khaibullin, B. I. Shtyrkov, M. M. Zaripov, R. M. Bayazitov, and M. F. Guljautdinov, *Radiat. Eff.* **36**, 225 (1978).

³B. C. Larson, C. W. White, T. S. Noggle, and D. Mills, *Phys. Rev. Lett.* **48**, 337 (1982).

⁴G. C. Bentini, C. Cohen, A. Desalvo, and A. V. Drigo,

Phys. Rev. Lett. **46**, 156 (1981).

⁵B. Stritzker, A. Pospieszczyk, and J. A. Tagle, *Phys. Rev. Lett.* **47**, 356 (1981).

⁶G. J. Galvin, M. O. Thompson, J. W. Mayer, R. B. Hammond, N. Paulter, and P. S. Peercy, *Phys. Rev. Lett.* **48**, 33 (1982).

⁷R. F. Wood and G. E. Giles, *Phys. Rev. B* **23**, 2923 (1981).

⁸J. A. VanVechten, R. Tsu, F. W. Saris, and D.

- Hoonhout, Phys. Lett. 74A, 417 (1979); J. A. VanVechten, R. Tsu, and F. W. Saris, *ibid.* 74A, 422 (1979); J. A. VanVechten, J. Phys. (Paris), Colloq. 41, C4-15 (1980).
- ⁹E. J. Yoffa, Phys. Rev. B 21, 2415 (1980).
- ¹⁰H. W. Lo and Compaan, Phys. Rev. Lett. 44, 1604 (1980).
- ¹¹R. M. Martin, Phys. Rev. Lett. 21, 536 (1968); Phys. Rev. 186, 871 (1969).
- ¹²V. Heine and J. A. VanVechten, Phys. Rev. B 13, 1622 (1976). See Eq. (5).
- ¹³A. M. Smirl, in *Proceedings of the NATO Advanced Study Institute: Physics of Non-Linear Transport in Semiconductors*, 1979, Vol. 52, p. 367.
- ¹⁴A. Elci, M. O. Scully, A. L. Smirl, and J. C. Matter, Phys. Rev. B 16, 191 (1977).
- ¹⁵J. M. Liu, R. Yen, H. Kurz, and N. Bloembergen, Appl. Phys. Lett. 39, 755 (1981).
- ¹⁶M. Combescot, Phys. Lett. 85A, 308 (1981).
- ¹⁷E. J. Yoffa, Phys. Rev. B 23, 1909 (1981).
- ¹⁸R. M. Pick, M. H. Cohen, and R. M. Martin, Phys. Rev. B 1, 910 (1970).
- ¹⁹S. L. Adler, Phys. Rev. 126, 413 (1962).
- ²⁰J. C. Phillips, *Covalent Bonding in Crystals, Molecules and Polymers* (University of Chicago Press, Chicago, 1969).
- ²¹J. M. Ziman, *Principles of the Theory of Solids*, 2nd ed. (Cambridge University Press, Cambridge, London, 1972).
- ²²D. Pines, *Elementary Excitations in Solids* (Benjamin, New York, 1964).
- ²³D. R. Penn, Phys. Rev. 128, 2093 (1962).
- ²⁴A. A. Maradudin, E. W. Montroll, G. H. Weiss, and I. P. Ipatova, *Theory of Lattice Dynamics in the Harmonic Approximation*, 2nd ed. (Academic, New York, 1971).
- ²⁵C. M. Bertoni, V. Bortolani, C. Calandra, and E. Tosatti, Phys. Rev. Lett. 28, 1578 (1972).
- ²⁶W. Weber, Phys. Rev. B 15, 4789 (1977).
- ²⁷V. Heine and J. A. VanVechten, Phys. Rev. B 13, 1622 (1976).
- ²⁸J. C. Phillips, *Bonds and Bands in Semiconductors* (Academic, New York, 1973).
- ²⁹B. A. Weinstein and G. J. Piermarini, Phys. Rev. B 12, 1172 (1975).